

# Effects of Glass Fabric and Laminate Construction on the Fatigue of Resin Infused Blade Materials

Daniel D. Samborsky, Pancasatya Agastra and John F. Mandell  
*Department of Chemical and Biological Engineering, Montana State University,*  
Bozeman, MT, 59717, USA

## Abstract

**New tensile fatigue test results are presented for infusion molded laminates, providing a comparison of several commercial E-glass reinforcing fabrics with epoxy resins over a range of fiber contents. Significant improvements in tensile fatigue resistance are demonstrated for some of the laminates relative to baseline materials, apparently depending on fabric architecture and stitching details. All stitched fabric laminates show a transition to lower fatigue resistance as the fiber content is increased, with the transition occurring at higher fiber content for the more fatigue resistant fabrics. The best fabric tested approached the performance of uniformly dispersed fiber prepreg molded laminates of similar construction. Differences in fatigue resistance appear to derive from the distortion and packing of fabric strands associated with increasing mold pressures, as demonstrated by finite element modeling and molding experiments at increasing pressures.**

## I. Introduction

Wind turbine blades experience very high numbers of fatigue cycles varying between tension, compression and reversed tension-compression loads, according to the particular loads spectrum for the turbine and wind conditions. The fatigue of composite laminates appropriate for wind turbine blades has been the topic of research studies for more than two decades. The findings of these studies are summarized in recent reports,<sup>1-3</sup> and in two current databases.<sup>4,5</sup> The most fatigue sensitive responses of typical glass fiber laminates are due to: (1) the tensile part of load cycles for the primary, axial load direction<sup>2,6</sup> and, (2) delamination between plies in the laminate at details such as spar/skin and trailing edge intersections, and ply drops used in thickness tapering.<sup>7,8</sup> This paper reports on new results related to the first area, exploring the effects on tensile fatigue response of variations in stitched glass reinforcing fabrics used in blade infusion processes.

## II. Background

The fatigue behavior of laminates based on a broad range of fabrics often used in hand lay-up processes has been reported.<sup>1,2,6</sup> Detailed analysis was presented for the effects of fiber content, fabric architecture, resin, and laminate construction parameters such as fiber orientation and fraction of plies in the axial (load) direction. This section provides a brief overview of these results as they apply to studies of current fabrics used in resin infusion. The resins used in most of the earlier studies were polyesters, but comparisons with vinyl esters and epoxies showed little effect on tensile fatigue.<sup>1,2</sup>

Figure 1 is a diagram and micrographs representing a unidirectional laminate containing D155 weft unidirectional stitched fabric (stitching not shown). The inter-strand areas are primarily neat resin, allowing for rapid wet-out. The intra-strand areas contain closely packed fibers with a continuous resin phase. At one extreme are fabrics with relatively large inter-strand channels, such as the D155 fabric. At the other extreme are laminates with no significant inter-tow areas, such as prepreg with uniformly dispersed fibers, which would appear entirely like the intra-strand micrograph. Current unidirectional infusion fabrics shown later tend to have large rectangular shaped strands which pack closely together, as well as small amounts of transverse strands or mat to which the main uni-strands are stitched; fiber contents can then approach typical prepreg values of 50-60% by volume, producing high stiffness and strength. Fabrics having fibers oriented in other directions, such as biax at  $\pm 45^\circ$ , can also be stitched to the uni ( $0^\circ$ ) strands to produce typical triaxial fabrics.

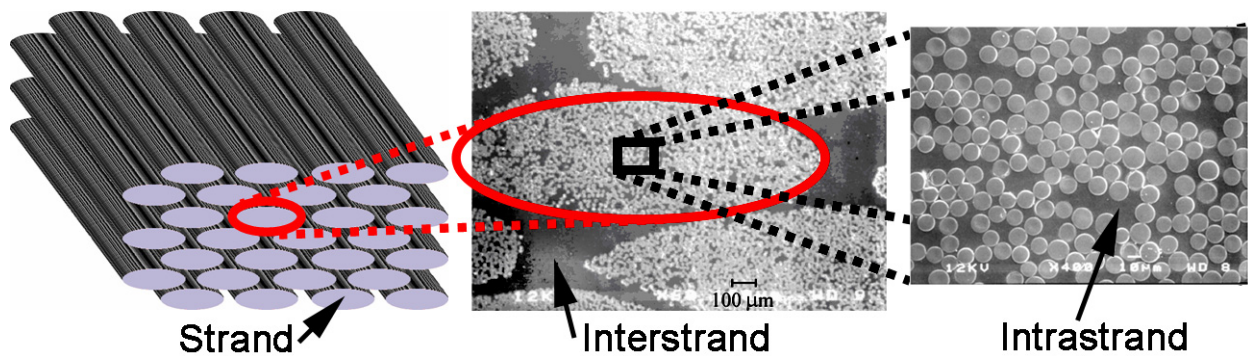


Figure 1. Exploded view of D155 Fabric A composite showing inter-strand channels and intra-strand structure.

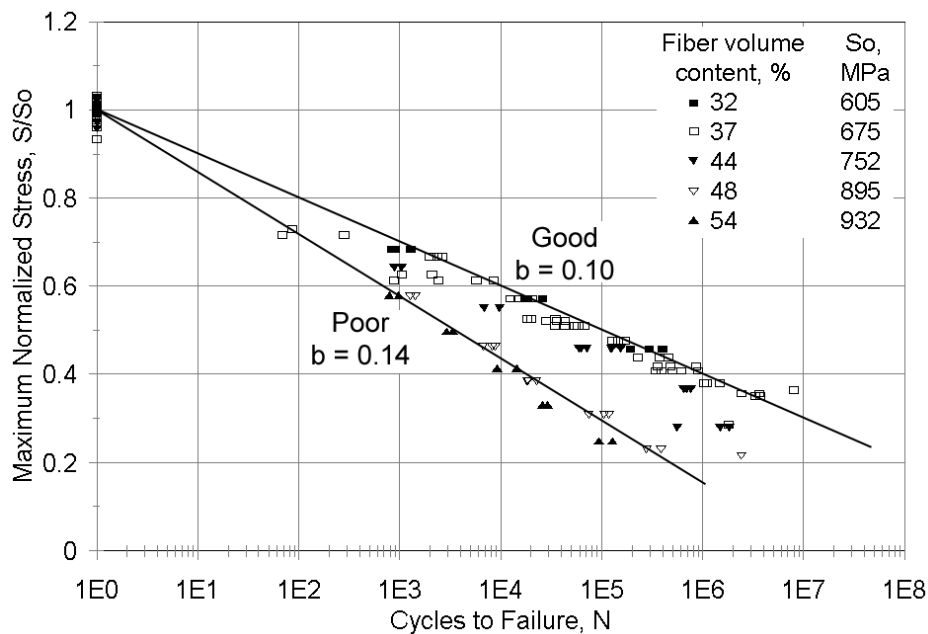


Figure 2. Normalized stress vs. log cycles to failure for DD-series E-glass/polyester laminates at various fiber contents, configuration [0/±45/0]s, R = 0.1.<sup>2</sup>

The D155 fabric was used in a variety of earlier studies as a baseline material, and compared with a broad range of stitched and woven fabrics from various manufacturers.<sup>1,2</sup> The results which follow are typical for fabrics with significant inter-strand channels, whether stitched or woven. Laminates in the DD series in the DOE/MSU Database<sup>4</sup> contain D155 0° fabric and DB120 biax ±45° fabric with a polyester resin. The fiber content was varied by controlling the spacing between the two-sided hard molds during RTM. Resin flow was primarily in-plane. Figure 2 gives typical S-N data for laminates with different fiber contents. The mean lifetime trend was fit with an exponential model

$$S/S_0 = 1.0 - b \log N \quad (1)$$

where S is the maximum tensile stress, S<sub>0</sub> the ultimate tensile strength at the fatigue load rate, N the cycles to fail (complete separation) and b is the slope of the normalized S-N curve. Tests were run at a constant R-value of 0.1, a typical tensile fatigue loading condition, where

$$R = \text{minimum load/maximum load} \quad (2)$$

The results from Figure 2 and similar laminates are plotted in Figures 3 and 4 as the slope of the S-N curves,  $b$ , and the maximum strain which can be sustained for a million cycles, respectively. As the fiber content increases above about 40% by volume, the S-N curves become significantly steeper and the million cycle strain decreases sharply. By both measures, the laminates become less fatigue resistant at higher fiber contents. This fatigue response is in contrast to the steadily increasing static strength,  $S_o$  (Fig. 2), and elastic modulus with increasing fiber content.<sup>1</sup> The typical triax fabric laminate shown in Figure 3 (based on CDB 200 fabric<sup>4</sup>) has poor fatigue resistance over the entire fiber content range, and fails along the stitch lines, where the local fiber content is high.<sup>1,2</sup> Laminates with low fiber content and associated good fatigue resistance shifted to poor resistance when flaws like ply drops were added, which caused local strand compaction and distortion.<sup>2</sup>

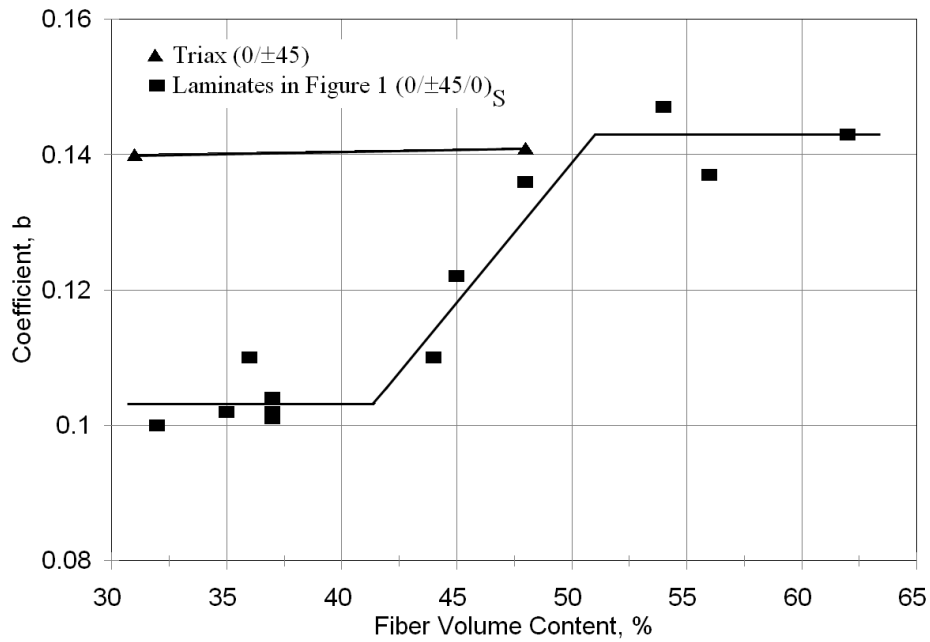


Figure 3. Fatigue coefficient,  $b$ , from Eq. (1) vs. fiber volume content for DD-series laminates,  $R = 0.1$ .<sup>2</sup>

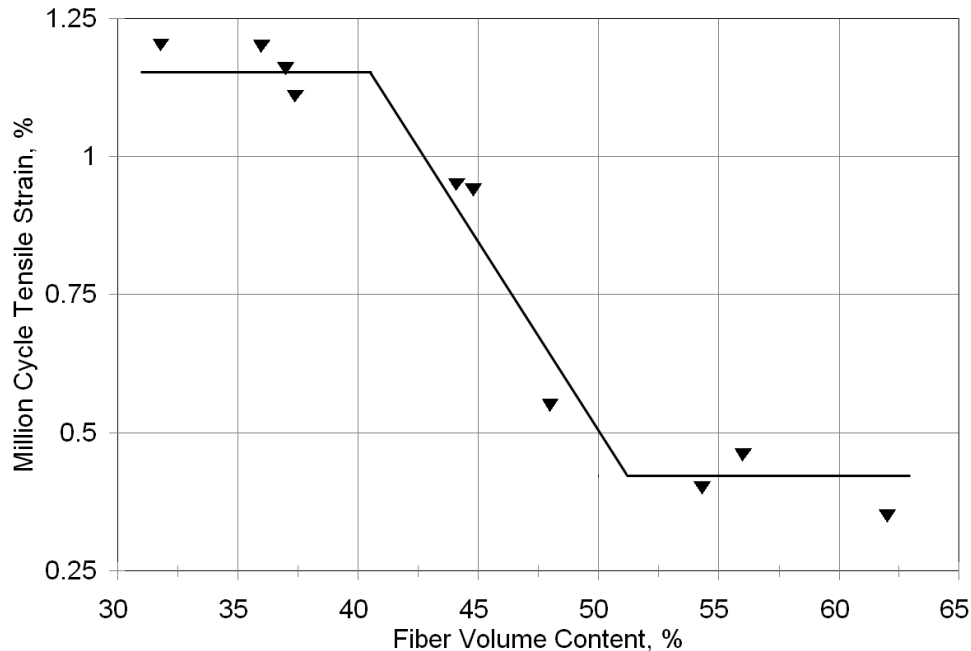
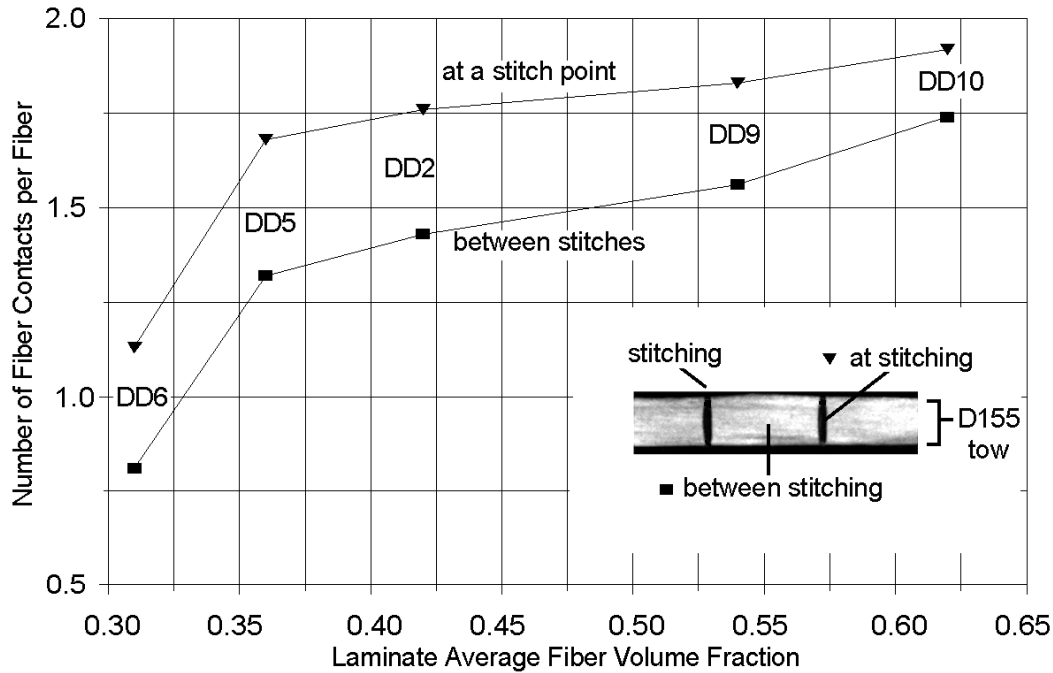


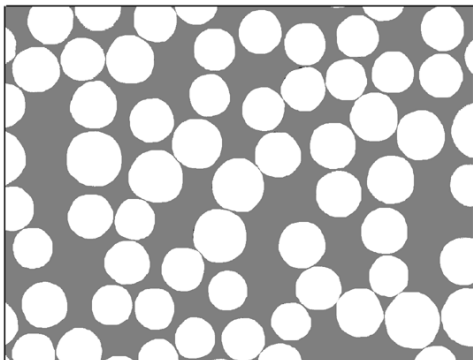
Figure 4. Million cycle tensile strain vs. fiber volume content for DD-series laminates,  $R = 0.1$ .<sup>2</sup>

The transition to poorer fatigue resistance at higher fiber contents has been associated with distortion and compaction of the strands as the fabric is squeezed at higher mold pressures. This produces very high local fiber contents within the strands, especially at stitch points, resulting in more fiber contacts, shown in Figure 5.<sup>2</sup> Mold pressure, strand distortion and fiber content are considered in detail later.

In essence a fabric, like the D155 in Figure 1, has an associated fiber content at low mold pressures as in vacuum bag molding. While compaction to higher fiber contents can be achieved by increasing the mold pressure, compressing the strands into the inter-strand (channel) areas, this results in poor fatigue performance. To achieve the higher properties associated with higher fiber contents while maintaining good fatigue resistance, the fabric architecture must be changed to reduce the inter-strand areas. This has been accomplished with many current infusion fabrics, as described later. A reduction in inter-strand channels has the negative effect of decreasing fabric permeability and ease of wet-out.



Micrograph of a D155 tow in a DD6 composite (micrograph local fiber volume fraction = 0.54)



Micrograph of a D155 tow in a DD10 composite (micrograph local fiber volume fraction = 0.67)

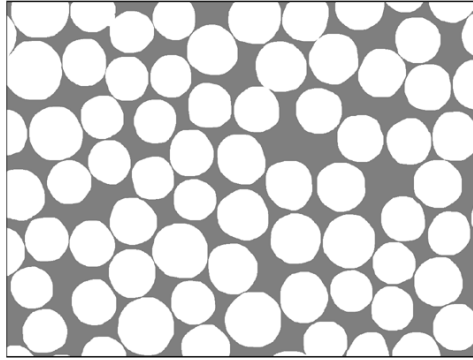


Figure 5. Number of contacts per fiber from neighboring fibers along stitch line and between stitch lines vs. average laminate fiber volume fraction, also showing micrographs (bottom) for intra-strand fiber packing, selected DD-series laminates.

### III. Experimental Methods and Data Reduction

#### A. Materials and Processing

Tensile fatigue results for laminates based on several fabrics, and with several resins, are presented. While most laminates used epoxy resin and some form of infusion process with fiber volume contents in the 50-60% range, results for infused polyester and vinyl ester resins, other fiber contents, and epoxy prepreg laminates are presented for comparison. The following is a description of the materials, where the material designation is taken from the current or future update of the DOE/MSU Fatigue Database.<sup>3</sup> Fabric details from manufacturers are listed in Table 1.

#### Materials List

1. DD Series (Fig's. 1-5). This is an early series of tests on E-glass/polyester laminates with 0° Fabric A and ±45° Fabric E.  
Lay-up and % 0°-material: [0/±45/0]<sub>s</sub>; 72%-0°  
Fiber volume fraction and thickness: both varied  
Matrix: polyester (CoRezyn 63-AX-051 with 1% MEKP)  
Process, cure and post-cure temperatures: VARTM, RT, 2 hours at 65°C  
Laminate fabricated by: MSU
2. QQ1. E-glass/epoxy laminate based on 0° Fabric B and ±45° Fabric F  
Lay-up and % 0°-material: [±45/0<sub>2</sub>]<sub>s</sub>, 64%-0°  
Fiber volume fraction and thickness: 0.53 and 4.09 mm  
Matrix: epoxy (Vantico TDT 177-155)  
Process, cure, and post-cure temperatures: VARTM, RT, 6 hours at 70°C  
Laminate fabricated by: MSU
3. QQ2. Same as QQ1 except lay-up [±45/0/±45]<sub>s</sub>,  $V_f = 0.52$ , thickness = 3.96 mm.
4. QQ4. E-glass/epoxy laminate based on 0° Fabric C and ±45° Fabric G  
Lay-up and % 0°-material: [±45/0/±45/0/±45]<sub>s</sub>, 56%-0°  
Fiber volume fraction and thickness: 0.57 and 4.03 mm  
Matrix: epoxy (Vantico TDT 177-155)  
Process, cure, and post-cure temperatures: VARTM, RT, 70°C  
Laminate fabricated by: MSU
5. QQ4-L. Same as QQ4 except  $V_f = 0.40$ , thickness = 5.70 mm
6. QQ4-M. Same as QQ4 except  $V_f = 0.46$ , thickness = 4.85 mm, resin is epoxy Prime 20LV with slow hardener, infused by VARTM at RT, post cured at 80°C
7. E-LT-5500-EP. E-glass/epoxy laminate based on 0° fabric D and ±45° Fabric G  
Lay-up and % 0° material: [±45/0/±45/0/±45]<sub>s</sub>, 66%-0°  
Fiber volume fraction and thickness: 0.55 and 4.59 mm  
Matrix: epoxy (Huntsman Araldite LY1564/hardener XB3485)  
Process, cure and post-cure temperature: Infusion (TPI SCRIMP<sup>TM</sup>), 60°C and 82°C  
Laminate fabricated by: TPI (Supplied by Global Energy Concepts/BSDS Program as material EL-T-5500/epoxy<sup>9</sup>)
8. E-LT-5500-VE. Same as E-LT-5500-EP except vinyl ester resin (Ashland Momentum 411-200),  $V_f = 0.55$ , thickness = 4.60 mm ( supplied by GEC as material EL-T-5500/VE<sup>9</sup>)
9. TT. Similar to E-LT-5500-EP except fabricated at MSU by VARTM, resin is Prime 20LV with slow hardener, infused at RT, post cured at 80°C,  $V_f = 0.55$ , thickness = 4.60 mm
10. TT1A. Same as material TT except ±45 fabric is Fabric F, resin is Vantico TDT 177-155, processed at RT by VARTM, post cured 6 hrs. at 70°C,  $V_f = 0.55$ , thickness = 4.37 mm

11. TT1AH. Same as material TT1A except  $V_f = 0.63$ , thickness = 3.98 mm
12. GGP4. Prepreg E-glass/epoxy (dispersed fibers in  $0^\circ$  plies)<sup>2</sup>  
 Lay-up and  $\%0^\circ$ -material:  $[\pm 45/0/\pm 45]$ , 50%- $0^\circ$   
 Fiber volume fraction and thickness: 0.53 and 1.9 mm  
 Prepreg:  $0^\circ$ -Hexcel M9.6/32%/1200/G;  $\pm 45^\circ$ -Hexcel M9.6/35%/BB600/G  
 Process and cure conditions: vacuum bag,  $90^\circ\text{C}$  for 12 hrs.  
 Laminate fabricated by: MSU
13. P2C. Prepreg E-glass/epoxy (dispersed fibers in  $0^\circ$  plies)  
 Lay-up and  $\%0^\circ$  material:  $[\pm 45/0_4]_s$ , 81%- $0^\circ$   
 Fiber volume fraction and thickness: 0.43 and 2.75 mm  
 Prepreg:  $0^\circ$ -Newport NCT-307-D1-E300 M1;  $\pm 45^\circ$ -NB307-D1-7781-497A (woven, cut at  $\pm 45$ )  
 Process and cure conditions: vacuum bag, 3 hrs. at  $121^\circ\text{C}$   
 Laminate fabricated by: MSU
14. SC1 Aligned strand unidirectional coupons machined from thick, megawatt scale blade spar-cap, E-glass/epoxy,  $V_f = 0.55$ , thickness = 5.0 mm

**Table 1. Fabric specifications ( from manufacturers).**

	Manufacturer	Designation	Fabric Weight, $\text{g/m}^2$	$\%0$	$\%45$	$\%90$	$\%RM$	$\% \text{Stitch}$
A	Knytex	D155	527	99	0	0	0	1
B	Saertex	U14EU920-00940-T1300-100000	955	91	0	8	0	1
C	Saertex	S15EU980-01660-T1300-088000	1682	97	0	2	0	1
D	Vectorply	E-LT-5500	1875	92	0	6	0	2
E	Knytex	DB120	393	0	97	0	0	3
F	Saertex	VU-90079-00830-01270-000000	831	0	97	2	0	1
G	Knytex	DBM-1708	857	0	68	0	30	2

## B. Test Methods

Grip related failure modes have been a problem at higher fatigue cycles with the short test specimens required for R-values containing compressive minimum loads, particularly for stronger materials with higher fiber contents and fractions of  $0^\circ$  material.<sup>3,6</sup> This study concentrated on tensile fatigue resistance, and tests were limited to  $R = 0.1$ , which allowed the use of reduced width, dog-bone shape specimens. Two specimen sizes were used as shown in Figure 6; the larger specimen has produced gage section failures in earlier studies<sup>6</sup>, and the smaller specimens were demonstrated to produce a consistent lifetime distribution, also with gage section failures. Figure 7 shows a typical failed specimens. The specimen size used for a particular test series can be found in the database;<sup>4</sup> essentially, all results presented are for gage section failures except for prepreg material P2C, which contained a very high  $0^\circ$  ply content. Also shown in Figure 6 is a thickness-tapered coupon for unidirectional material SC1, which produced gage section failures.

Static tests were run under displacement controlled ramp loading at a similar rate to the fatigue tests, 13 mm/s. The rate can have a significant effect on static strength for glass fiber materials as described elsewhere, with values usually on the order of 15% higher at typical fatigue displacement rates than at standard static test rates.<sup>6</sup> Fatigue tests were run under sine-wave, load control, constant amplitude. The frequency was varied approximately inversely with maximum load to maintain a constant load rate; individual test frequencies are given in the DOE/MSU database.<sup>4</sup> Frequencies were in the 1-10 Hz range to avoid significant heating; surface temperatures were monitored for selected tests, and fatigue specimens were surface cooled with fans.<sup>1,2</sup> Failure in all cases was taken as complete separation of the test coupon, although significant matrix cracking in the  $\pm 45^\circ$  plies was readily observable well before failure, often on the first fatigue cycle (Figure 8).

Fatigue strains were measured on the first few cycles of the test using an extensometer. The strains are only representative of the first few cycles, and increase gradually as damage accumulates under controlled stress.<sup>1,2</sup> The elastic modulus was determined at a slow rate using an extensometer.

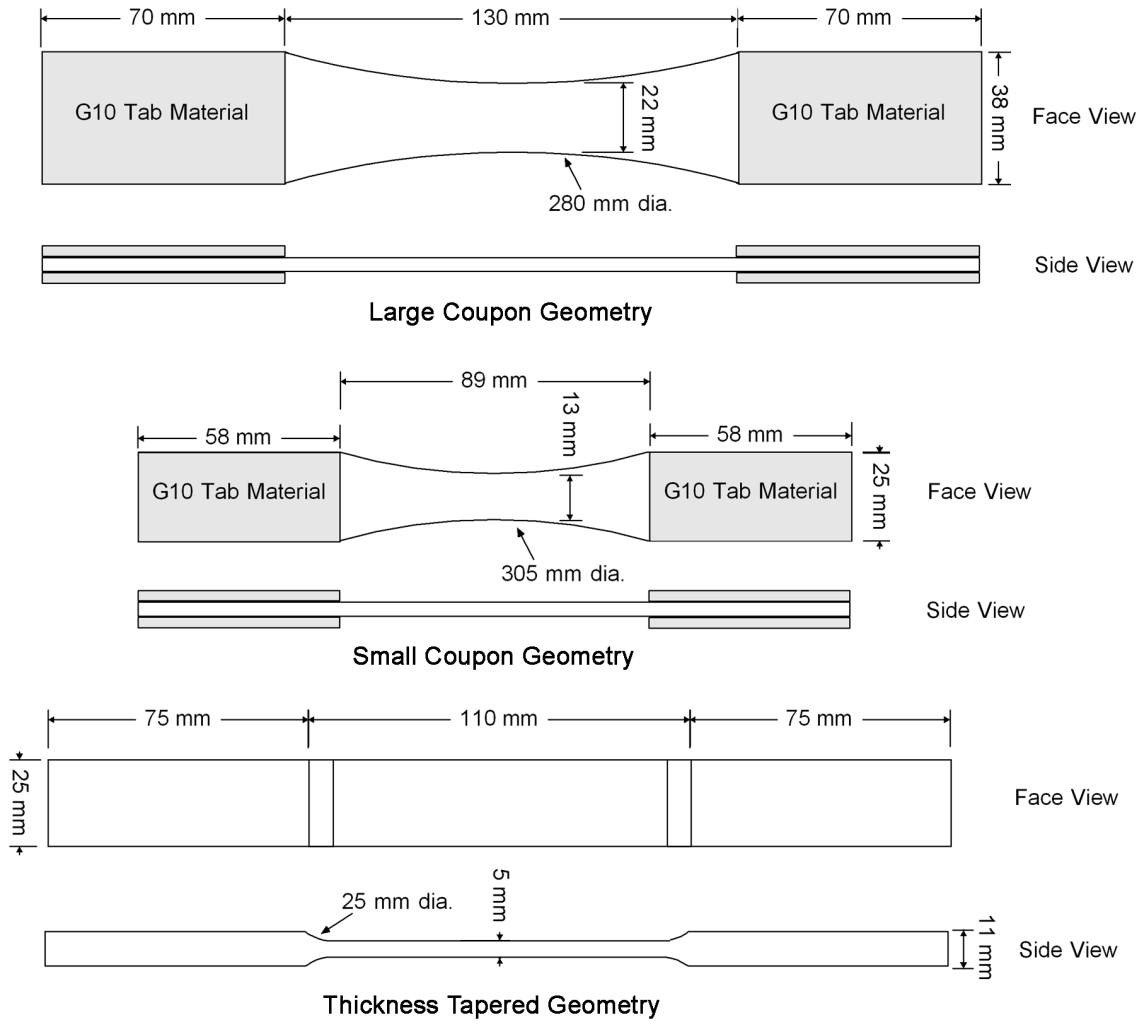


Figure 6. Coupon geometries.

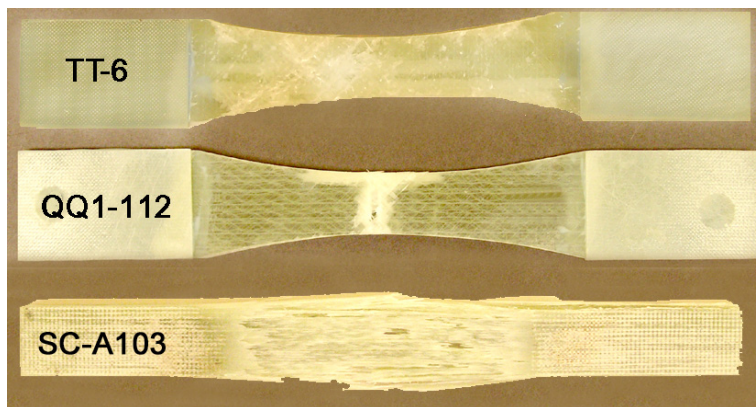


Figure 7. Failed fatigue specimens of QQ1, TT1A and SC1 materials.

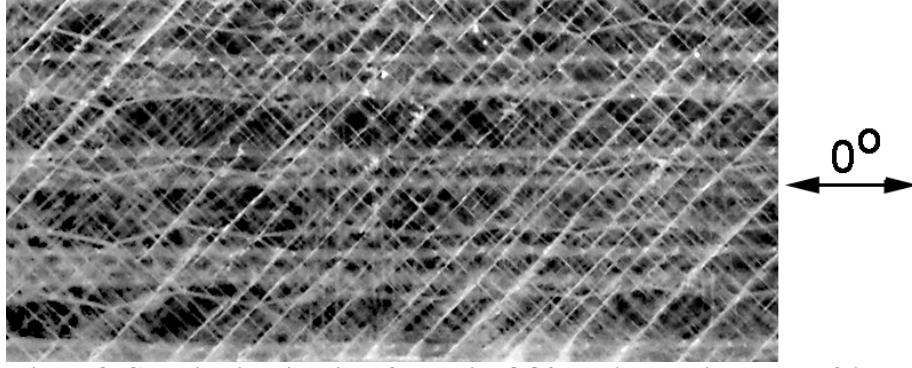


Figure 8. Cracking in  $\pm 45^\circ$  plies of material QQ2 specimen prior to total failure.

### C. Data Reduction

Static data are reported as mean tensile elastic modulus, tensile strength and ultimate tensile strain, each for at least three test specimens. The modulus value was determined at a slow rate in tension, fit to stress-strain data for a strain range between 0.1% and 0.3%. The ultimate strain value was determined from an extensometer. The fatigue strains were measured with an extensometer on the first few cycles for a particular test, and are best considered initial strain values. As more cycles accumulate at the constant loads used for each test, the strain gradually increases, but measurement difficulties preclude continuous monitoring.<sup>1-3</sup> The fatigue strain values determined from measured initial strains tend to be moderately higher than strains calculated through the tensile modulus for the tests run at higher maximum stresses.<sup>9</sup> Actual accumulated strains at failure would be even higher.

Fatigue results are represented with the power law model in Eq. (3), which provides a better fit to most data-sets at high cycles than does the exponential model in Eq. (1).<sup>2,3,6</sup> Static data were not included in the curve fits as discussed elsewhere, so low cycle lifetimes are not well represented for some cases.<sup>6</sup> The fits given here are for mean lifetime; more complete statistical representation is given elsewhere for several of the materials.<sup>3,6</sup> The value of stress or strain at  $10^6$  cycles is then taken from the fit equation as a basis for comparing the tensile fatigue resistance of different laminates as discussed later.

$$S = A N^B \quad (3)$$

where S is the maximum stress or strain, N is cycles to failure, and A and B are constants.

## IV. Results and Discussion

### A. Static Properties

Laminate elastic modulus and ultimate strength and strain are listed in Table 2. The laminates include differing contents of  $0^\circ$  and  $\pm 45^\circ$  material given in Table 1, so the static modulus and strength will reflect variations in construction as well as fiber content. The static ultimate strains show less sensitivity to laminate construction as long as there is a significant  $0^\circ$  content, but laminate quality, stitching and fiber alignment do affect ultimate strain. The QQ4 series of laminates show somewhat higher strength and modulus as compared to the E-LT-5500 EP, apparently due to the higher  $0^\circ$  fiber content of Fabric C as compared to Fabric D. The lower weight Fabric B produces lower ultimate strains than QQ4, apparently associated with the smaller strands. Other static property differences appear to relate to the overall fraction of  $0^\circ$  material in the laminates (see the materials list).

**Table 2. Average static data and fatigue fit parameters.**

Material	Static Tensile Strength, MPa	Ultimate Tensile Strain, %	Elastic Modulus, GPa	10 <sup>6</sup> cycle strain, %	Eq. (3) Mean Fit Parameters			
					Strain		Stress	
					A	B	A	B
QQ1	843	2.56	33.1	0.47	3.494	-0.1447	1121	-0.1425
QQ2	552	2.50	23.3	0.63	3.731	-0.1288	734.6	-0.1216
QQ4	986	3.10	31.8	0.59	3.589	-0.1313	1048	-0.1263
QQ4L	673	3.13	21.5	1.15	4.474	-0.0983	939.4	-0.0979
QQ4M	790	3.09	25.6	0.76	5.038	-0.1372	1071	-0.1284
E-LT-5500-EP	837	3.36	29.4	0.89	5.322	-0.1301	1264	-0.1208
E-LT-5500-VE	809	2.47	30.5	0.72	4.624	-0.1344	1146	-0.1384
TT	858	2.96	29.0	0.84	5.309	-0.1336	1523	-0.1327
TT1A	899	3.24	27.7	0.97	3.965	-0.1023	1176	-0.1093
TT1AH	930	2.95	31.5	0.63	3.694	-0.1279	1163	-0.1301
GGP4	817	3.03	27.9	1.08	5.314	-0.1156	1256	-0.1108
P2C	869	3.20	27.0	1.48	3.897	-0.0700	1116	-0.0762
SC1	924	2.30	40.0	0.86	2.232	-0.0692	977.9	-0.0785

## B. Fatigue Results

Tensile fatigue results are presented in Figures 9-11 for the materials listed earlier. In each case the data are presented in terms of both maximum stress and maximum strain vs. log cycles to failure for  $R = 0.1$  (Eq. 2). As noted earlier, the stress is controlled to be constant over the duration of the test, while the strain is the maximum initial strain taken over the first few cycles, after which the extensometer is removed. The fatigue data (not including static, one cycle values) are fit to Eq. (3), with the fit parameters given in Table 2; the fits are for mean lifetime.

Figure 9 gives the results for laminates with 0° Fabrics B and C, which differ by a factor of two in weight and thickness. Material QQ1, with four stacked 0° plies, has been the subject of earlier studies under a variety of loading conditions,<sup>6</sup> while in material QQ2 each 0° ply is separated by  $\pm 45^\circ$  plies; little difference in fatigue strains is evident between the two. Materials QQ4, QQ4-L and QQ4-M, representing high (57%), low (40%), and medium (46%) fiber contents, contain the heavier 0° Fabric C, and the  $\pm 45^\circ$  plies, Fabric G, include a layer of mat. While the static strength and modulus increase with fiber content as expected, only the lowest fiber content laminate shows good fatigue resistance in terms of strains. The materials based on 0° Fabric D, shown in Figure 10, have consistently good fatigue resistance in terms of strain, except for the highest fiber content, material TT1A-H (63% fiber volume content). Materials TT and E-LT-5500 EP contain  $\pm 45^\circ$  Fabric G, with mat, while Materials TT1A and TT1A-H contain Fabric F, without mat. The similarity of Materials TT and TT1A indicates that the presence of mat with the  $\pm 45^\circ$  plies has little effect on tensile fatigue strains.

The results in Figure 11 are presented for comparison to the infused fabric results in Figures 9 and 10. Materials in Figure 11, GGP4 and P2C were fabricated from E-glass/epoxy prepregs and contain 0° plies with well dispersed fibers as opposed to stitched strands. The prepreg plies are all relatively thick, and the processing was by vacuum bag, to be representative of blade materials (see materials list). Both of the prepreg based materials show high fatigue strains. The unusually low fiber volume content and eight stacked 0° plies for material P2C may be responsible for its unusually high strain values. Also shown on Figure 11 is Material SC1, unidirectional E-glass/epoxy fabricated from aligned strands, and having well dispersed fibers. Test specimens were cut from a megawatt scale blade spar cap supplied by a blade manufacturer. Sectioning of the thick spar cap to obtain test coupons (Figures 6 and 7) may result in some damage such as cut fibers; also, testing of unidirectional materials often creates grip interaction problems.<sup>1-3</sup> However, these coupons with thickness tapering failed mostly in the gage section, and the fatigue strains in Figure 11 are fairly good.

The data in Figures 9-11 are for epoxy resin systems given in the materials list. Material E-LT-5500 has been tested with vinyl ester (VE) as well as epoxy (EP). Both materials were infused by TPI using their SCRIMP™

process, and have the same fabrics and approximate fiber contents. Figure 12 indicates that the fatigue stresses and strains are moderately higher for the epoxy matrix as compared with the vinyl ester. This difference is consistent with the static strength and ultimate strain values in Table 2. Earlier studies with DD series materials at lower fiber contents had shown no significant differences between epoxy, vinyl ester and polyester resin laminates.<sup>1</sup>

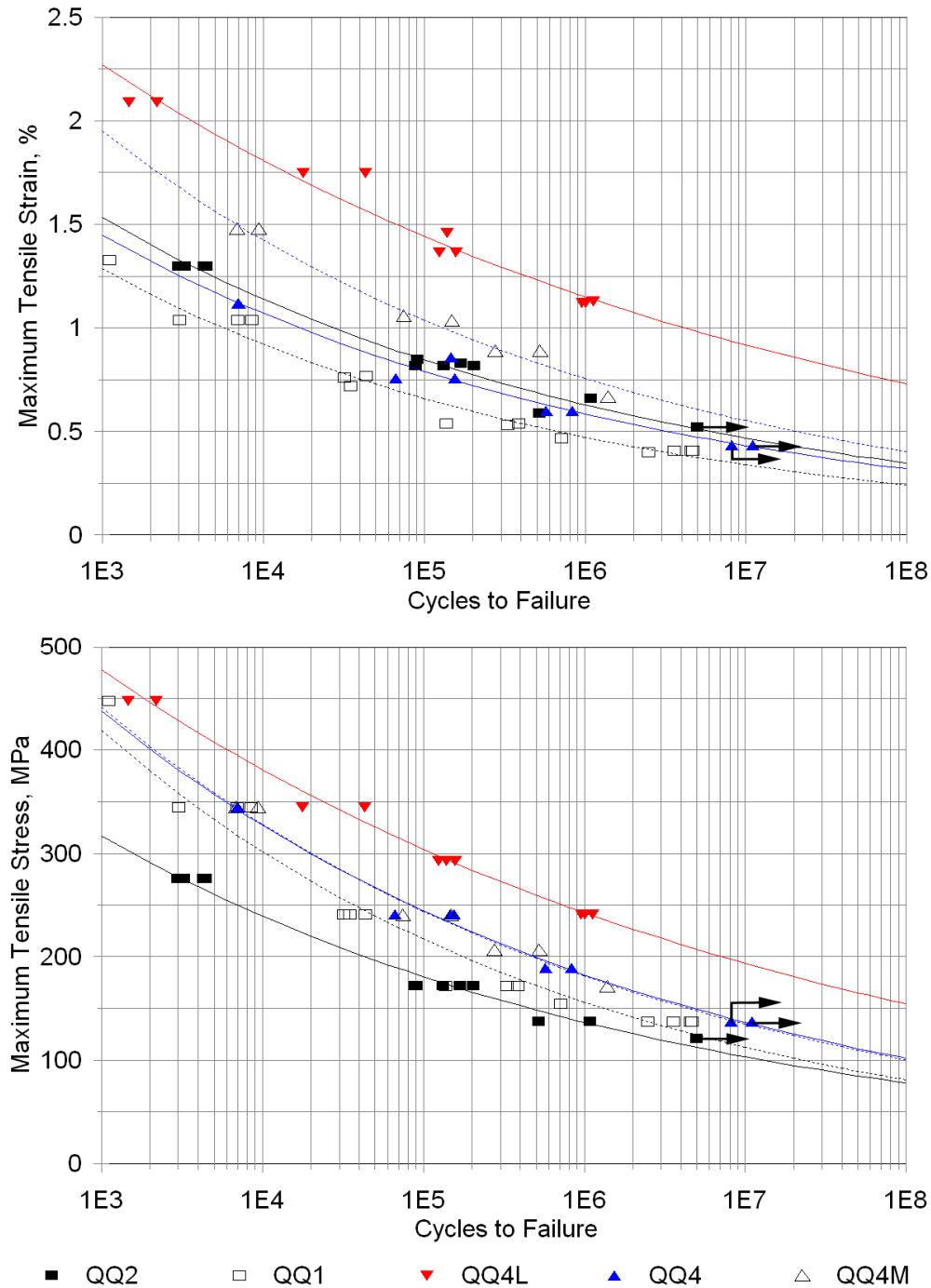
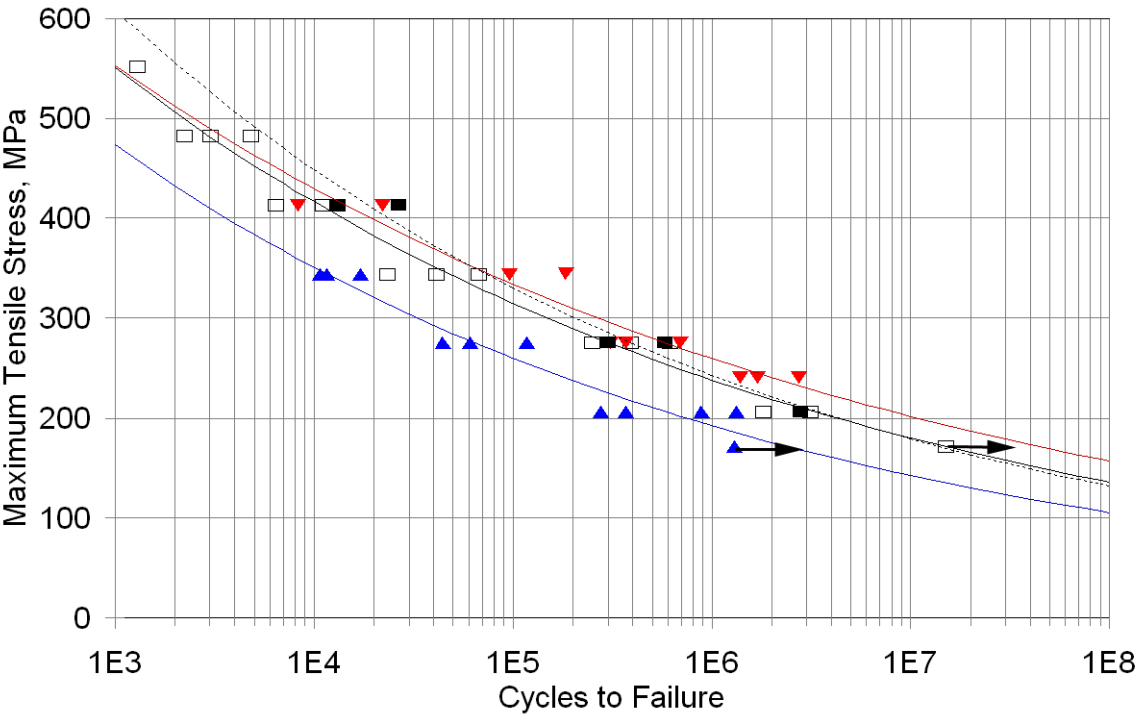
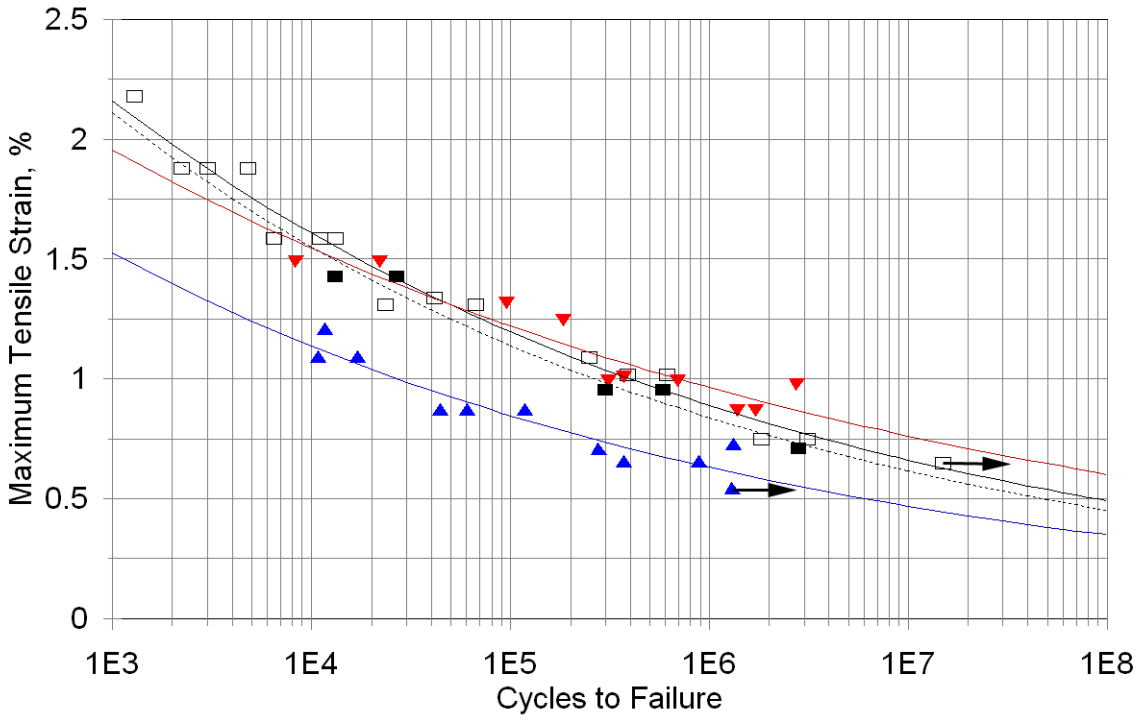


Figure 9. Maximum strain (top) and maximum stress vs. log cycles to failure for materials QQ1 and QQ2, based on Fabric B, and materials QQ4, QQ4L and QQ4M, based on Fabric C, R = 0.1.



E-LT-5500-EP
  TT1A
  TT1AH
  TT

Figure 10. Maximum strain (top) and stress vs. log cycles to failure for materials TT, TT1A, TT1A-H and E-LT-5500-EP, based on Fabric D, R = 0.1.

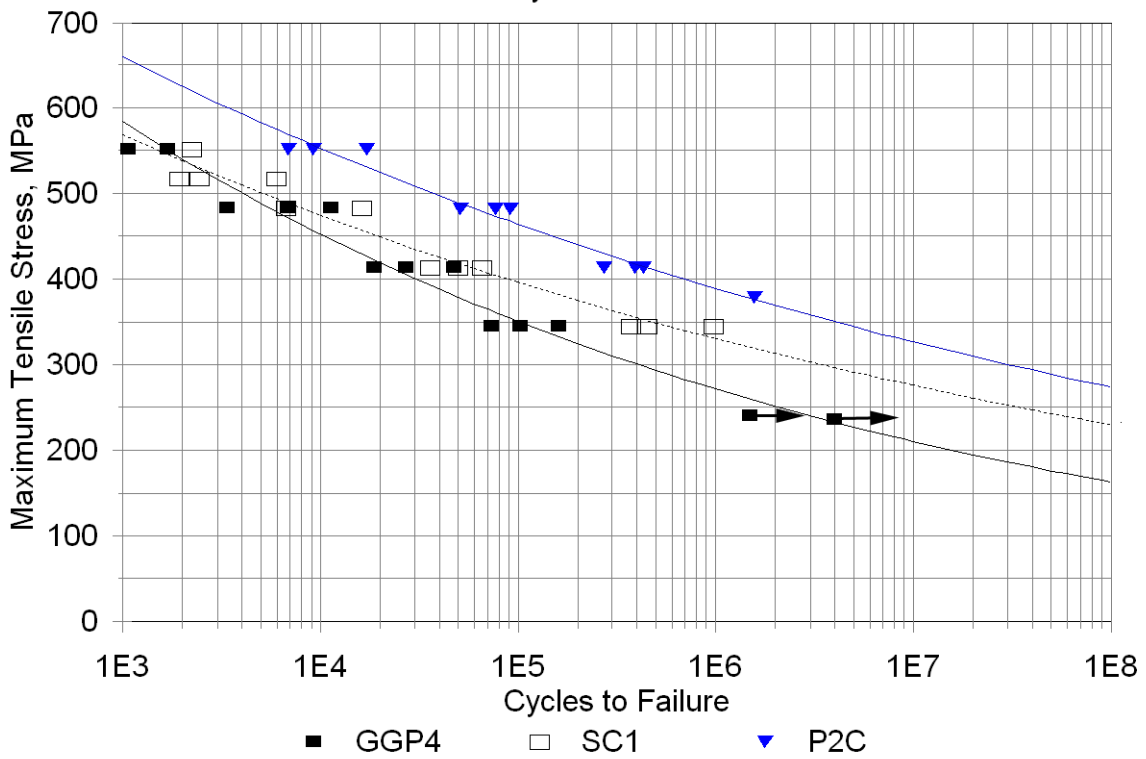
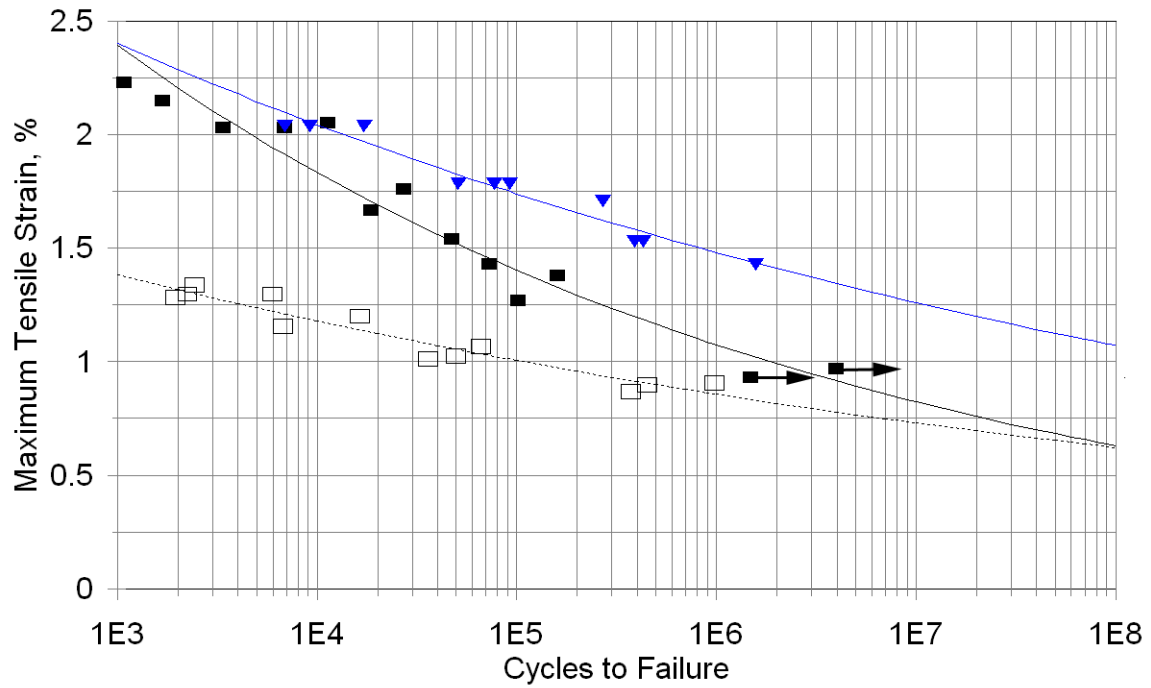


Figure 11. Maximum strain (top) and maximum stress vs. log cycles to fail, prepreg materials GGP4 and P2C, and spar-cap material SC1,  $R = 0.1$ .

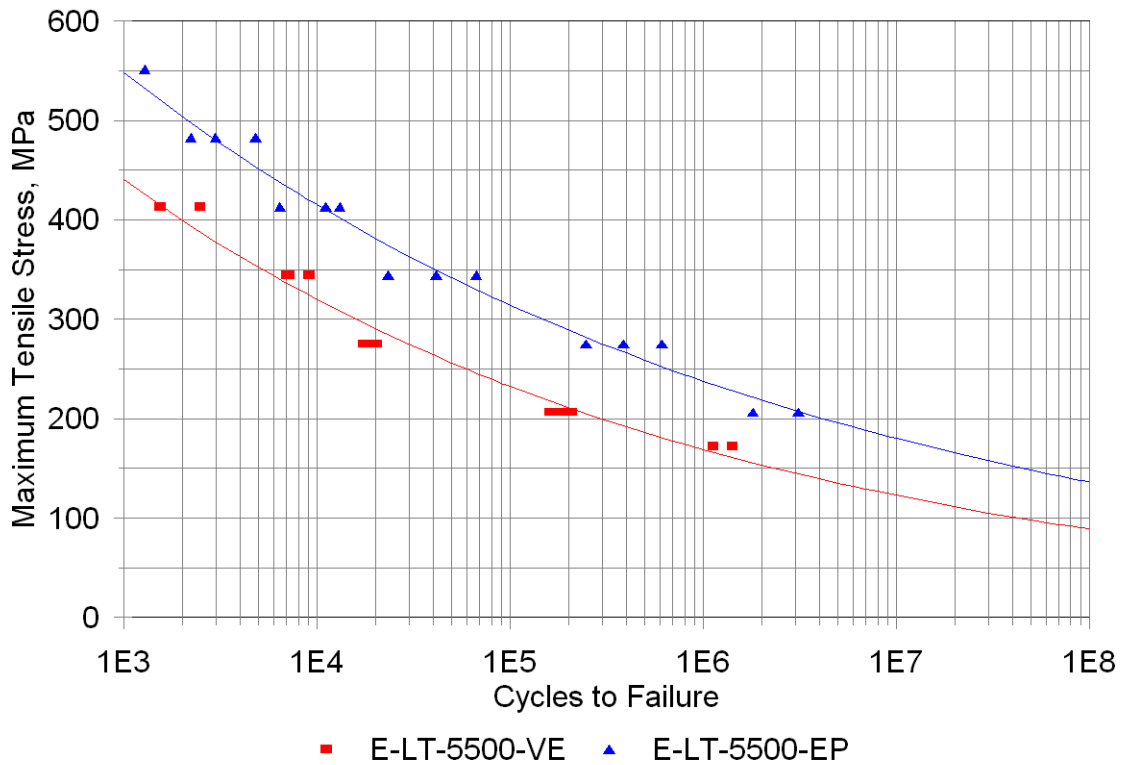
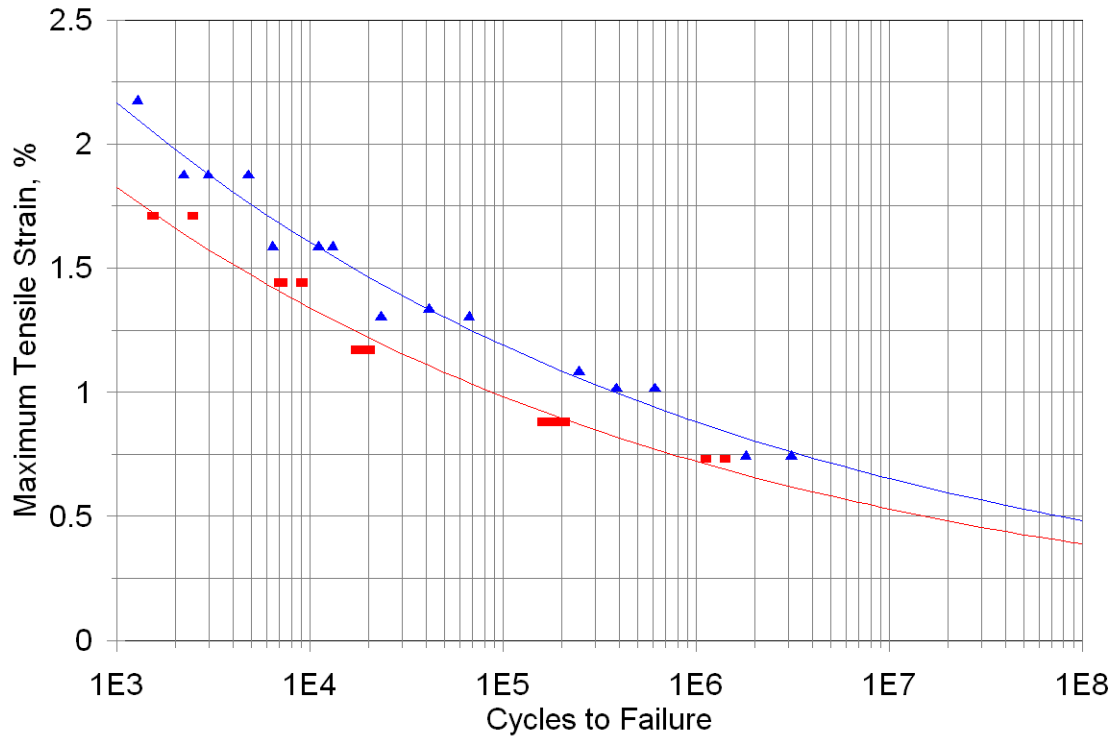


Figure 12. Comparison of maximum strain vs. log cycles to fail data for material E-LT-5500 EP (epoxy resin), and E-LT-5500 VE (vinyl ester resin), R = 0.1.

### C. Analysis of Fabric Effects

Different materials based on different reinforcing fabrics (see the materials list) are compared in terms of the maximum tensile fatigue strain which can be withstood for a million cycles, determined from the curve fits in Table 2. This follows the approach in Figure 4;<sup>2</sup> other measures of fatigue resistance such as the exponents of the S-N fits in Table 2 would show consistent trends. The results in Figure 13 show a marked difference between laminates based on the different 0° fabrics tested. (Note that many other commercial fabrics from different manufacturers are available, but were not included in this study.) The general trend of the results is clear for the DD Series laminates based on Fabric A. As noted earlier, as the fiber content increases (as determined by the mold opening in the VARTM process with hard molds on both sides), the fatigue resistance as represented by the million cycle strain decreases rapidly above about 40% fiber by volume. The strain capacity at higher fiber contents drops to less than half the value at lower fiber contents. At the other extreme, materials based on Fabric D retain good fatigue resistance to above 55% fiber by volume, then drop above 60% fiber. These results approach those shown for prepreg laminates. Fabric C in the QQ4 Series laminates is very similar in construction and weight to Fabric D, but shows a transition to lower fatigue resistance at much lower fiber contents, close to Fabric A. The lighter weight but otherwise similar Fabric B (materials QQ1 and QQ2) shows even lower fatigue strains than Fabric C.

It should be noted that the ±45° plies form extensive matrix cracking prior to total laminate failure. The more fatigue resistant 0° Fabric D sustains extreme visible matrix damage and ply delamination prior to failure, which would likely be unacceptable in service. Definitions of failure may need revision for the more fatigue resistant materials.

The differences in materials such as QQ4 (Figure 9) and TT and E-LT-5500 EP (Figure 11) at similar fiber contents and overall fabric specifications is pervasive over entire panels and for different batches, with different processors. This difference is illustrated in the direct comparison in Figure 14. No individual fatigue test results for the more fatigue sensitive materials approach the worst performing specimens from the less fatigue sensitive materials at the same strain level. This despite similar static properties. Thus, the increase in fatigue sensitivity is not due to some form of occasional flaw, but is inherent in the gage section of every test specimen.

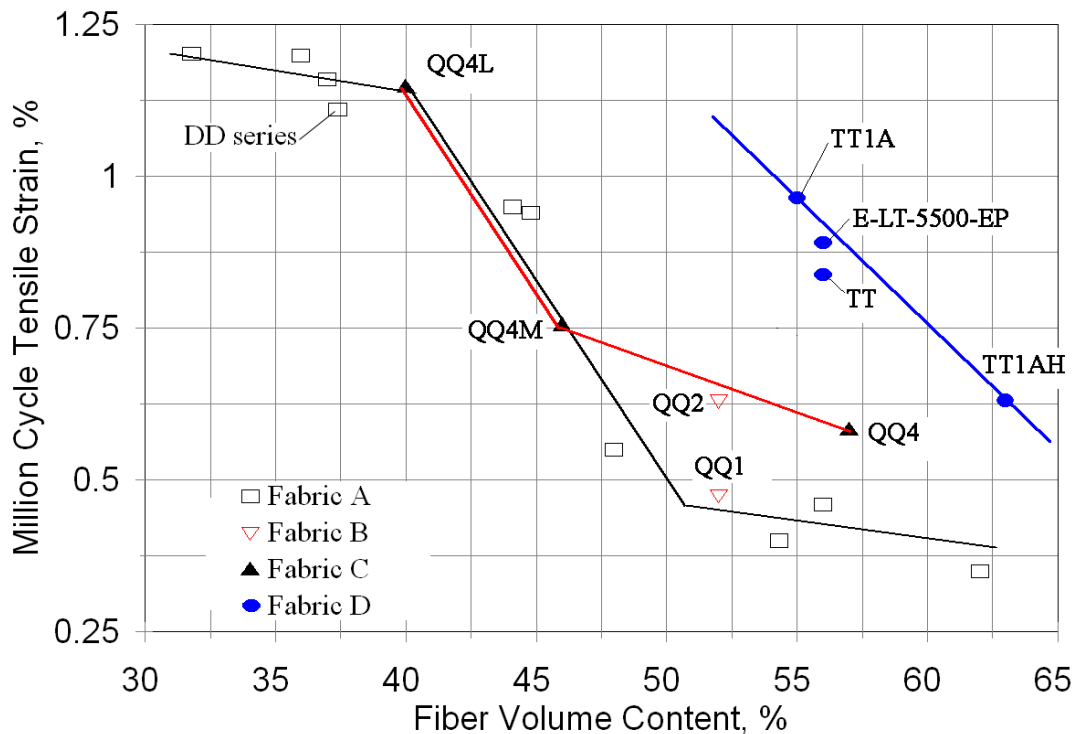


Figure 13. Million cycle strain vs. fiber volume content for various infused materials showing transitions to reduced fatigue resistance as a function of 0° fabric, R = 0.1.

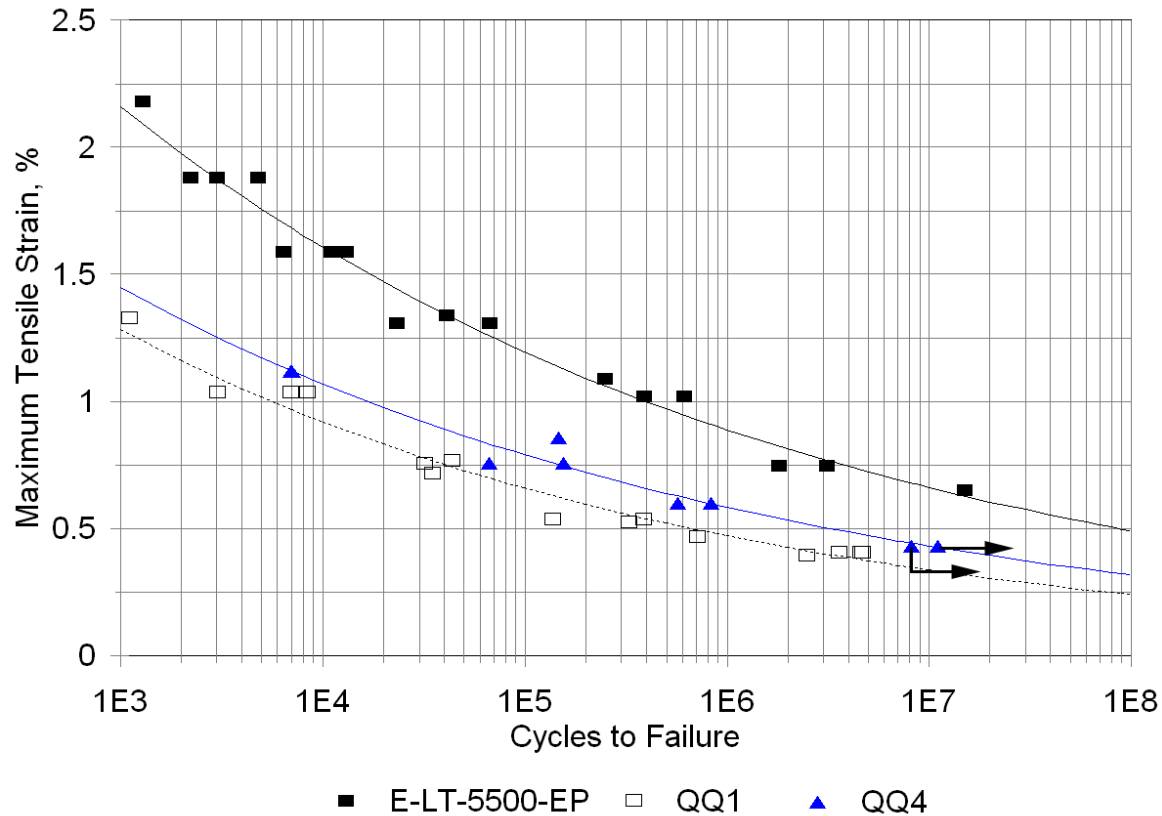


Figure 14. Direct comparison between materials QQ1, QQ4 and E-LT-5500-EP in terms of maximum strain vs. cycles to fail,  $R = 0.1$ .

Fabrics C and D are very similar in construction, given in Table 1. In cross-section, these fabrics are densely packed compared with Fabric A due to their rectangular strand cross-sections and large strands, with small inter-strand areas (Figure 1). Figure 15 gives cross-sections of Materials QQ4 and TT;  $\pm 45^\circ$  plies, stitching, and  $90^\circ$  strands to which  $0^\circ$  strands are stitched can also be seen in the photographs (Table 1). The fiber content as a function of mold pressure has been determined (Figure 16) for Fabrics A, C, and D, following methods described elsewhere.<sup>2</sup> Fabrics C and D are very similar in terms of the fiber content reached as a function of mold pressure, while Fabric A reaches much lower fiber contents for the same pressure. At low pressure conditions like 10-20 kPa, Fabric A fiber content is around 40%, while Fabrics C and D are around 55% fiber by volume; these ranges are typical of hand lay-up vs. infusion processes for which the fabrics are apparently designed. Transitions to poor fatigue resistance occur as the fiber content is raised above the low pressure range for Fabrics A and D, but at a lower fiber content for Fabric C.

Figure 17 is taken from a current study of fabric distortion during molding, modeled by finite element analysis. A frictional interaction is assumed between strands and at strand/mold interfaces. The deformed and un-deformed cases are shown for Fabric A, which has initially elliptical strand cross-sections and large inter-strand spaces (Figure 1). Significant strand shape and local fiber content changes occur<sup>2</sup> as the mold opening is decreased, and the inter-strand channel area decreases, decreasing the fabric permeability.<sup>10</sup> The rectangular strands of Fabrics C and D are already at a high fiber content before molding, as shown.

The origin of the relatively poor fatigue performance for Fabrics B and C appears to be related to the details of stitching rather than the strand content. Fabric D is stitched with larger stitching, has a higher stitch content, and the strands appear to be held more straight in the fabric batches examined to date. There appears to be more spreading of the strands between stitches in some areas for Fabrics B and C than for Fabric D. However, further study is needed.

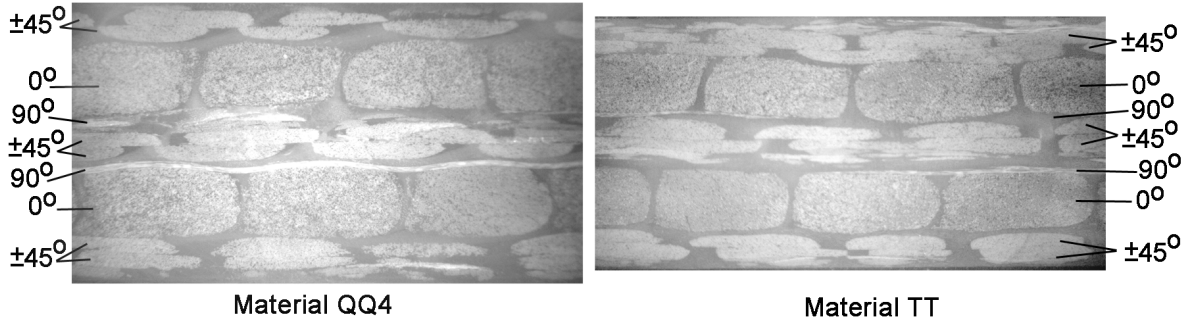


Figure 15. Comparison of cross-section views of laminates QQ4 (Fabric C), and TT (Fabric D).

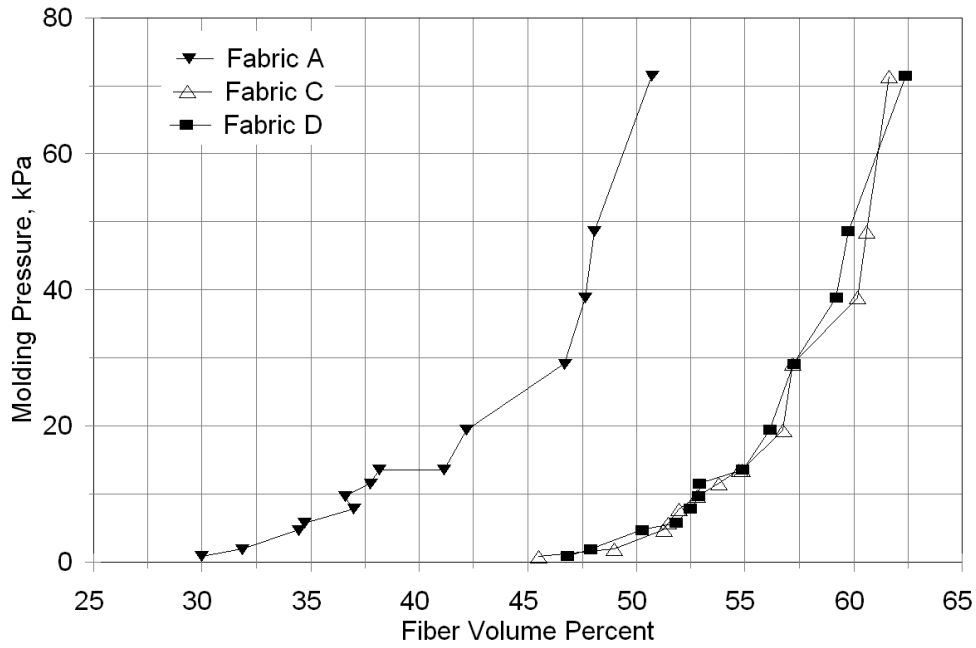


Figure 16. Mold pressure vs. fiber content for Fabrics A, C, and D, measured for [0<sub>2</sub>] laminates.

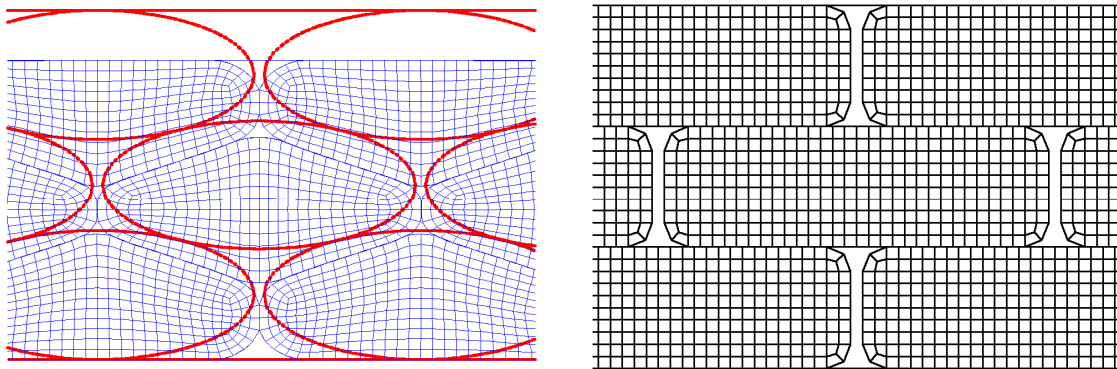


Figure 17. Finite element models for Fabric A (left) and Fabric D (right); the left side illustrates fabric distortion from the original elliptical strands (red) to distorted strands (black) as the mold pressure increases.

## V. Conclusions

Marked differences are demonstrated in the tensile fatigue resistance for infused laminates based on stitched glass fabrics having very similar fabric specifications, laminate construction, fiber content, resin and processing. Laminates based on Fabric D consistently outperform those based on Fabrics B or C, despite similar static properties. The transition to increased fatigue sensitivity occurs above 55% fiber by volume for Fabric D materials, below 45% for Fabrics B and C. Typical infused blade laminates have fiber contents around 50-55% fiber by volume, so Fabric D is clearly preferred. Fatigue strain levels for laminates based on Fabric D approach those for typical prepreg based laminates at high cycles. Coupons cut from an aligned strand unidirectional megawatt scale blade spar cap (without stitching) approached the performance of Fabric D based laminates despite likely effects of machining. Vinyl ester resin produced somewhat reduced static and tensile fatigue performance relative to otherwise identical material with epoxy resin for laminates infused by the TPI SCRIMP™ process with Fabric D.

## VI. Acknowledgements

This work was funded by Sandia National Laboratories under subcontract Z3609. Prepreg materials were supplied by Newport Adhesives and Composites and Hexcel, and E-LT-5500 laminates were supplied by Global Energy Concepts through the BSDS program.<sup>9</sup>

## References

- <sup>1</sup> Mandell, J.F., and Samborsky, D.D., "DOE/MSU Composite Material Fatigue Database: Test Methods, Materials, and Analysis," Contractor Report SAND97-3002, Sandia National Laboratories, Albuquerque, NM, 1997.
- <sup>2</sup> Mandell, J.F., Samborsky, D.D., and Cairns, D.S. "Fatigue of Composite Materials and Substructures for Wind Turbine Blades," Contractor Report SAND2002-0771, Sandia National Laboratories, Albuquerque, NM, 2002.
- <sup>3</sup> Nijssen, R.P.L. "Fatigue Life Prediction and Strength Degradation of Wind Turbine Rotor Blade Composites," PhD. Thesis, Delft University, the Netherlands, 2006, (ISBN -10190-9021221-3); (Also Sandia Contractor Report SAND2006-7810P, Sandia National Laboratories, Albuquerque, NM, 2006.)
- <sup>4</sup> Mandell, J.F., and Samborsky, D.D., DOE/MSU Fatigue of Composite Materials Database. 2006 Update. (<http://www.sandia.gov/wind/other/973002upd0306.pdf>)
- <sup>5</sup> Nijssen, R.P.L., "OptiDAT - Fatigue of Wind Turbine Blade Materials Database," 2006, ([www.kc-wmc.nl/optimat\\_blades](http://www.kc-wmc.nl/optimat_blades)).
- <sup>6</sup> Samborsky, D. D., Wilson, T. J. and Mandell, J. F., Proc. 2007 ASME Wind Energy Symposium, Paper AIAA-07-67056, AIAA/ASME, Reno, NV, 2007.
- <sup>7</sup> Samborsky, D., D., Avery, D. P., Agastra, P., and Mandell, J. F., Proc 2006 ASME Wind Energy Symposium, Paper AIAA-2006-1195, AIAA/ASME, Reno, NV, 2006.
- <sup>8</sup> Wilson, T.J., "Modeling of In-Plane and Interlaminar Fatigue Behavior of Glass and Carbon Fiber Composite Materials," MS Thesis, Department of Mechanical Engineering, Montana State University, 2006.
- <sup>9</sup> Global Energy Concepts, "Blade System Design Study Part II: Final Project Report," Sandia Contractor Report, in press.
- <sup>10</sup> Cairns, D. C. and Mastbergen, D., Proc. 2006 ASME Wind Energy Symposium, Paper AIAA-2006-1201, AIAA/ASME, Reno, NV, 2006.